ELSEVIER

Journal of Power Sources 104 (2002) 201–207

JOURNAL OF POWER SOURCES

www.elsevier.com/locate/jpowsour

Effects of F-treatment on degradation of Mg_2Ni electrode fabricated by mechanical alloying

Jun Sung Kim*, Chang Rae Lee, Jae Woong Choi, Sung Goon Kang

Division of Material Science and engineering, Hanyang University, 133-791 Seoul, South Korea

Received 19 June 2001; accepted 31 August 2001

Abstract

The effects of surface fluorination on the electrochemical charge–discharge properties of a Mg_2Ni electrode, prepared by mechanical alloying in Ni-MH batteries are investigated. After 20 h milling, Mg and Ni powder form nanocrystalline Mg_2Ni. The discharge capacity of this alloy increases greatly on the initial cycle but, due to the formation of a $Mg(OH)_2$ passive layer, displays rapid degradation in alkaline solution within 10 cycles. In a 6 M KOH+x M KF electrolyte ($x = 0.5$, 1, and 2), a continuous and stable fluorinated layer is formed and the durability of the Mg_2Ni electrode increases marketly and a high rate discharge capability is obtained (90–100 mAh/g). Addition of 2 M KF leads to the highest durability of all the electrodes tested. The improvement is due to a thin MgF_2—flourinated layer, which reduces the charge-transfer resistance and protects the Mg_2Ni electrode from forming a $Mg(OH)_2$ layer.

Keywords: Hydrogen storage materials; Nanostructures; Mechanical alloying

1. Introduction

Recently, there have been extensive studies on Ni-MH batteries for electric vehicle (EV) and the hybrid electric vehicle (HEV) applications because of the high specific energy of there batteries [1,2]. Nevertheless, still higher specific energy is required for the commercialization of Ni-MH batteries. Nowadays, the negative electrode is made from AB_5 and AB_2 type alloys but many investigations have shown that the specific capacity is still unsatisfactory because of the large specific gravity of these alloys. Therefore, A_2B type alloys such as Mg_2Ni are considered to be more promising materials for hydrogen storage since they have the highest hydrogen storage capacity (3.6 wt.%), light weight and low cost because of their relative abundance from sea bitterns. In addition, the theoretical discharge capacity of Mg_2Ni is high, i.e. about 1000 mAh/g, compared with other alloys [3]. In spite of these good characteristics, the Mg_2Ni-type electrode has several disadvantages [4–8], namely:

1. sluggish hydriding/de-hydriding kinetics at room temperature;
2. low electrochemical discharge capacity at room temperature;
3. low diffusion rate of hydrogen;
4. easy oxidation in alkaline solution;
5. high charge-transfer resistance to hydrogen redox reactions at the electrode/electrolyte interface.

In order to improve the above problems, much research has been conducted and the following electrode preparation techniques have been proposed: mechanical alloying (MA) [9], micro-encapsulation [10,11], F-treatment [12–14], heat-treatment [15], alloying with other elements [16,17], and composite structures [18,19]. Nevertheless, the practical electrochemical capacity of Mg_2Ni-type alloy is still less than that of other types of metal hydride alloys.

According to Liu et al. [13], fluorinated surface structures have significant benefits in terms of rapid hydrogen uptake, and exhibit strong resistance against gaseous and liquid impurities. By mechanical alloying, Woo and Lee [9] have synthesized a Mg_2Ni electrode which has good low-temperature characteristics.

The purpose of this work is to study the effect of fluorination on the degradation of nanocrystalline Mg_2Ni electrode and to investigate the relationship between electrochemical corrosion behavior and performance by automatic galvanostatic charge–discharge testing and electrochemical impedance spectroscopy (EIS).

* Corresponding author.
E-mail address: kayjune@hanmail.net (J.S. Kim).

0378-7753/02/$ – see front matter
PII: S0378-7753(01)00917-X

2. Experimental

2.1. Preparation of alloys and electrodes

Mg-Ni hydrogen storage alloys were synthesized by a MA process. The MA process was performed with a SPEX 8000-D ball-mill. The starting materials for ball-milling were elemental powders of Mg (99.8% pure, less than 175 μm) and Ni (Inco 255, less than 45 μm). The materials were placed in a hardened steel vial together with two steel balls of 1/2 in. and four of 3/8 in. in diameter. The atomic ratio of Mg to Ni was 2:1, and the ratio of powder to balls was 1:5, in weight. The handling of powder was undertaken in an argon-filled glove box to avoid oxidation.

The electrodes were fabricated by mixing the alloy powder synthesized by MA with pure Ni powder in a weight ratio of 1:2, and then cold pressing into a pellet of 10 mm in diameter under a pressure of 5 t/cm^2.

2.2. Characterization of alloys and electrodes

The microstructure of alloys were analyzed by X-ray diffraction (XRD) using Cu Kα radiation ($\lambda = 1.5418$Å, Regaku D-MAX 3000) and transmission electron microscope (TEM, JEM-2010). The phase changes of electrodes and surface morphologies before and after cycle tests also were examined by XRD, scanning electron microscope (SEM),and energy dispersion spectrum (EDS), respectively. To investigate the oxidized state of the electrode surfaces, auger electron spectroscopy (AES, PHI-680, Auger nanoprobe, sputtering rate is 98 Å/min SiO_2/Si) was used. The dissolution of the active materials after 1, 3, 5, 7, and 10 cycles was investigated by means of induced coupled plasma atomic emission spectroscopy (ICP–AES, JY 1380 Ultra ICP).

2.3. Electrochemical charge–discharge test

All electrochemical cycle tests were carried out with a half-cell which consisted of the hydrogen storage alloy as a working electrode, a platinum mesh as a counter electrode, and a mercury/mercurous oxide (Hg/HgO) as a reference electrode in 6 M KOH electrolyte (K electrolyte) and 6 M KOH electrolyte with x M KF electrolyte ($x = 0.5$, 1, and 2; 0.5, 1, and 2F electrolyte) at room temperature. The electrochemical charge–discharge cyclic tests were performed using an automatic galvanostatic charge–discharge unit (Maccor series 4000) at constant current of 10, 20, and 100 mA/g. Total charging current was 400 mA/g. The discharge cut-off voltage was set −0.6 V with respect to the reference electrode. The resting time between charge and discharge was 5 min.

2.4. Electrochemical impedance measurement

The electrochemical impedance measurements were carried out in the half-cell described above. The electrolytes were K electrolyte and xF ($x = 0.5$, 1, and 2) electrolyte. The electrochemical impedance was measured by means of EG&G Princeton Applied Research (PAR) electrochemical impedance analyzer (Model 6310) controlled by electrochemical impedance software (M398) with an IBM-PC computer. The electrochemical impedance spectra (EIS) of the metal hydride electrode were recorded over the frequency range 10 mHz–100 kHz using a 5 mV ac amplitude of perturbation. All measurements of electrochemical impedance were taken at 0% depths-of-discharge (DOD) and at ambient temperature.

3. Result and discussion

3.1. Characteristics of ball-milled Mg_2Ni powders

X-ray diffraction patterns of ball-milled Mg-Ni powder with 0 and 20 h milling times are given in Fig. 1. After 20 h ball-milling, broad Mg_2Ni peaks appear. This is due to the stored energy from mechanical stress in the grains and refinement of the average grain size [20]. The ball-milled alloy had a nanosized crystalline structure, as shown in the TEM micrographs given in Fig. 2. The electronic diffraction pattern reveals that a Mg_2Ni phase is formed and that the average grain size is less than 20 nm in the dark-field image.

3.2. Electrochemical test and rapid degradation

The electrochemical charge–discharge cyclic life of the nanocrystalline Mg_2Ni and arc-melted Mg_2Ni are compared in Fig. 3. The initial discharge capacity of the nanocrystalline Mg_2Ni phase (280 mAh/g) greatly improved compared with that of the polycrystalline counterpart (20 mAh/g). The powder obtained by the MA method has many defects in the

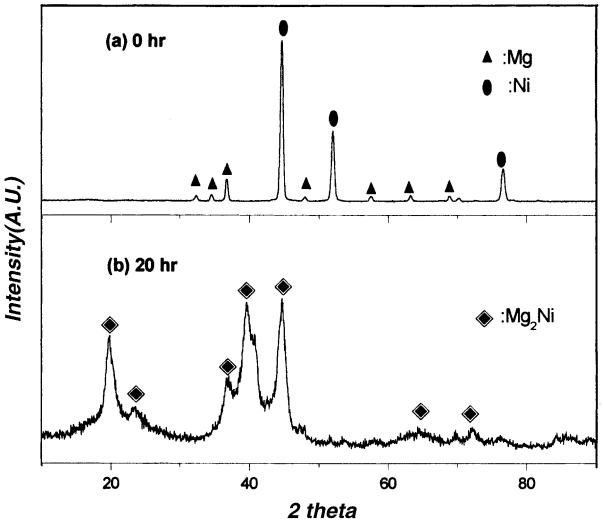

Fig. 1. X-ray diffraction patterns of ball-milled Mg_2Ni for (a) 0 h and (b) 20 h.

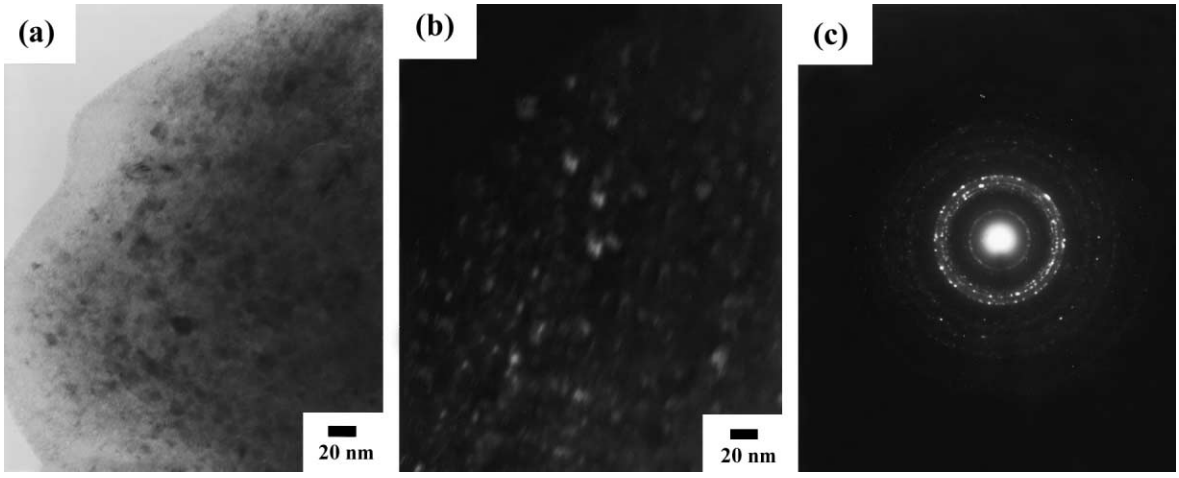

Fig. 2. TEM images of 20 h ball-milled Mg_2Ni (a: bright field image, b: dark field image, c: diffraction pattern image).

crystal and also a larger grain size, which may help to increase the number of hydrogenation sites and the rate of diffusion for hydrogen.

Rapid degradation still remains a problem with nanocrystalline Mg_2Ni electrode. The surface of the electrode after 10 cycles is covered with a thick oxide layer, as shown by the AES depth profile in Fig. 4. The magnesium hydroxide layer can be formed easily on the surface of the Mg alloy in alkaline electrolyte, even in the potential of hydrogen evolution, because the standard potential of magnesium is lower than the equilibrium hydrogen potential [24]. The hydroxide film on the metal surface is produced by the reduction of water according to the following corrosion reactions:

$$\text{Anodic reaction}: \quad Mg \rightarrow Mg^{2+} + 2e^- \tag{1}$$

$$\text{Cathodic reaction}: \quad 2H_2O + 2e^- \rightarrow 2OH^- + H_2 \tag{2}$$

$$\text{Overall reaction}: \quad Mg + 2H_2O \rightarrow Mg(OH)_2 + H_2 \tag{3}$$

This reaction of magnesium hydroxide can occur during both the charge and the discharge process. The magnesium hydride formed during charge may also be oxidized to magnesium hydroxide by water according to following reactions:

$$MgH_2 \rightarrow Mg(\text{act}) + 2H^+ + 2e^- \tag{4}$$

$$Mg(\text{act}) \rightarrow Mg^{2+} + 2e^- \tag{5}$$

$$2H_2O + 2e^- \rightarrow 2OH^- + H_2 \tag{6}$$

$$MgH_2 + 2H_2O \rightarrow Mg(OH)_2 + 2H_2 \tag{7}$$

The absorption and desorption reaction of hydrogen results in a volume change of the metal hydride. This would make a more active surface of magnesium than non-hydride metal. The reaction of hydroxide formation of magnesium hydride would be accelerated on repetitive charge–discharge

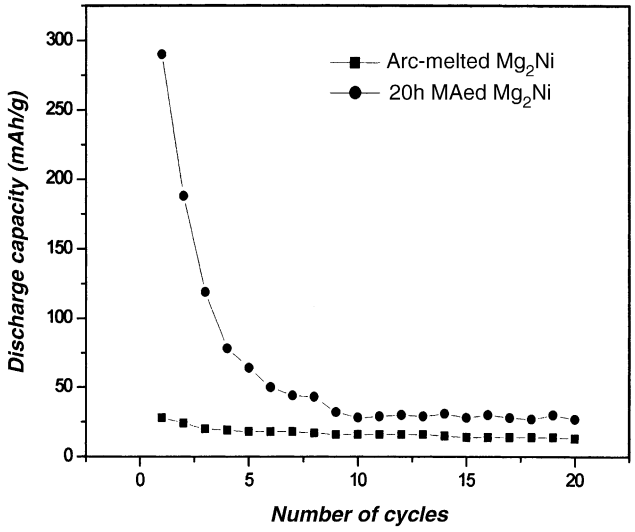

Fig. 3. Discharge capacities of (a) arc melted and (b) 20 h ball-milled Mg_2Ni electrode.

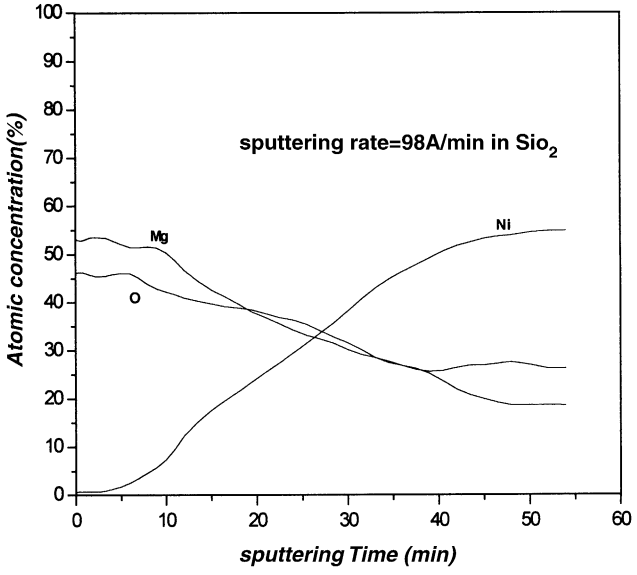

Fig. 4. AES depth profile of cycled electrode after 10 cycles in K electrolyte.

cycling. The current of the corrosion reaction would contribute to the initial discharge capacity of ball-milled metal hydride electrode.

We consider that the thick hydroxide layer formed during charge–discharge cycling prohibits hydrogen from diffusing in or out through the electrode surface and eventually causes rapid degradation. Also, the defects in the alloy which result from ball-milling accelerate the formation of the hydroxide layer and thus cycle-life decreases rapidly.

3.3. Effect of fluorination treatment

In order to lower the rate of degradation of electrodes, in situ surface modification is performed by adding an aqueous fluorine-containing solution which is made by mixing xF ($x = 0.5$, 1, and 2) electrolyte [13]. The electrochemical discharge properties of a Mg_2Ni electrode with K and x M KF electrolyte are shown in Fig. 5. Although loss of initial maximum discharge capacity, the durability of Mg_2Ni electrode with fluorine-containing electrolyte is greatly increased. In this test, the electrolyte with 2 M KF has the best durability of all those tested here. The ratio of capacity to maximum capacity of a Mg_2Ni electrode with/without 2 M KF electrolyte is given in Fig. 6. It has been reported [4] that the ratio of discharge capacity to the maximum capacity in K electrolyte can be decreased to lower than 20% of the maximum capacity. By contrast, the electrode after 2 M F-treatment has over 70% of the maximum capacity after 10 cycles.

For a discharge current of 100 mA/g, the discharge capacity of the Mg_2Ni electrode in electrolyte with or without 2 M KF is compared in Fig. 7. The cycle-life of the electrode in 2F electrolyte is greater than that in K electrolyte.

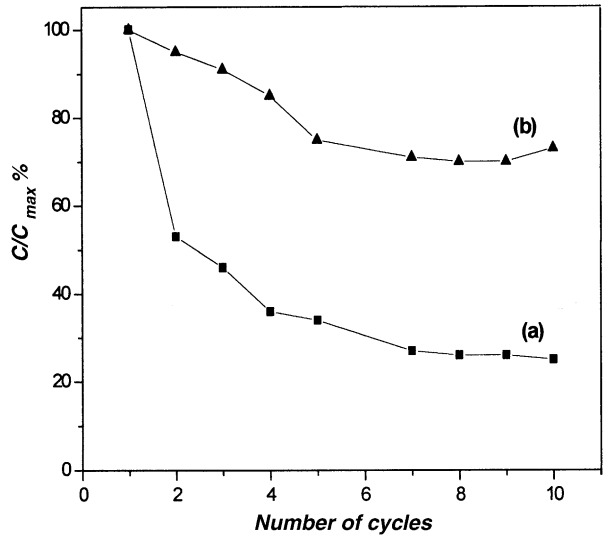

Fig. 6. Ratio of capacity to maximum capacity of Mg_2Ni electrode in different electrolyte (a) K electrolyte and (b) 2F electrolyte.

3.4. Effect of F-treatment on Mg_2Ni degradation and durability

In general the degradation of the Mg_2Ni electrode can be summarized as follows [21] During the discharge process, the Mg_2Ni electrode is very corrodible in alkaline solution, therefore Mg from the hydrogen storage alloy diffuses out of the Mg_2Ni phase and reacts with OH^- from the electrolyte to form a passive $Mg(OH)_2$ layer. This $Mg(OH)_2$ phase acts as a passive layer for hydriding and de-hydriding. Also, the layer increases the reaction resistance at the electrode surface. Consequently, the voltage of the cell falls.

With a F-containing electrolyte which forms a MgF_2 layer, which is sufficiently porous to allow diffusion porous

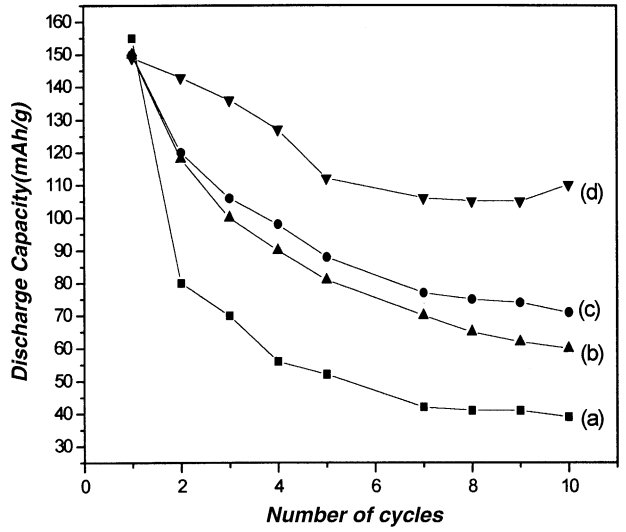

Fig. 5. Discharge capacities of Mg_2Ni electrode for 20 mA/g discharge; (a) K electrolyte, (b) 0.5F electrolyte, (c) 1F electrolyte, (d) 2F electrolyte.

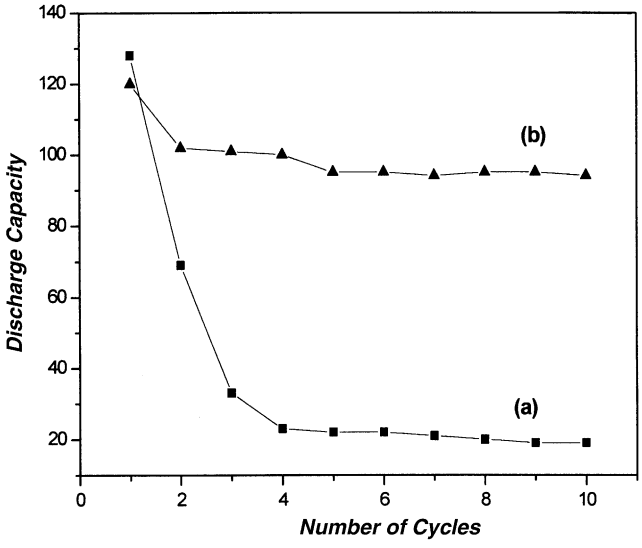

Fig. 7. Discharge capacities of (a) K electrolyte and (b) 2F electrolyte for 100 mA/g.

of hydrogen, but not for OH^- ions. Even though the conductivity of the electrolyte is decreased somewhat [22], the cycle-life of the electrode could be increased. This is because, during the hydriding and the de-hydriding process, the formation of MgF_2 is superior to that of $Mg(OH)_2$, as listed in Table 1 [23].

Since Mg has very low heat of formation changes (ΔH_f), it reacts very easily with O_2 and H_2O onto the surface. A MgO phase is produced in the outer layer and a Ni-rich phase in the inner layer of alloy. The MgF_2 layer can protect the electrode from forming a passive layer because the formation reaction of MgF_2 is more stable thermodynamically than that of $Mg(OH)_2$ or MgO. Furthermore, it could remove

Table 1
Standard formation enthalpy and equilibrium constant of compounds

Compounds (ΔH_f° kJ/mol)	Enthalpies (log K_f)	T (K)	Equilibrium constant
MgH_2	−79.099 to −76.149	298.15–600	−0.413 to 6.432
MGO	−706.844 to −601.241	298–3105	99.677–1.677
$Mg(OH)_2$	−924.664 to −923.070	298–542.2	73.156–146.051
MQF_2	−1124.241 to −1244.556	298–1536	28.612–187.653

$Mg(OH)_2$ and MgO via the following reactions.

$$MgO + 2H^+ + 2F^- = MgF_2 + H_2O \quad (8)$$

$$Mg(OH)_2 + 2H^+ + 2F^- = MgF_2 + 2H_2O \quad (9)$$

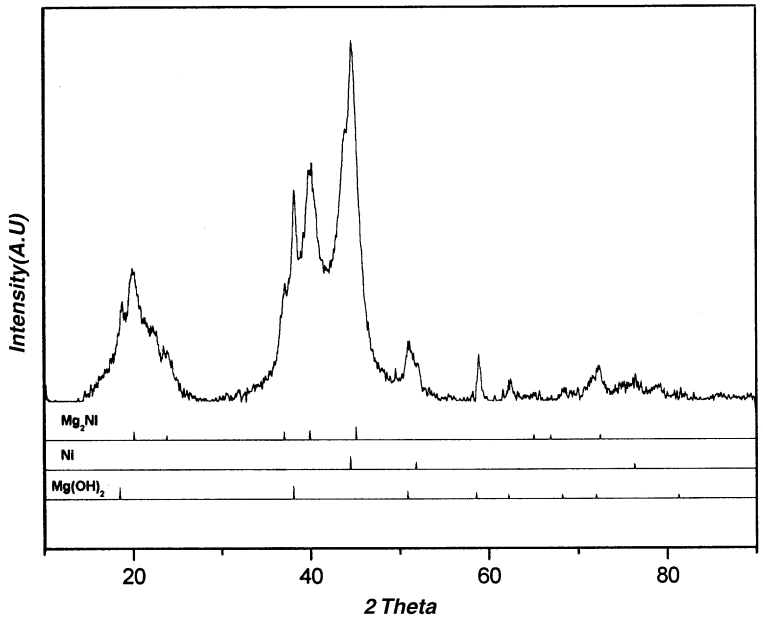

Fig. 8. XRD pattern of Mg_2Ni in K electrolyte.

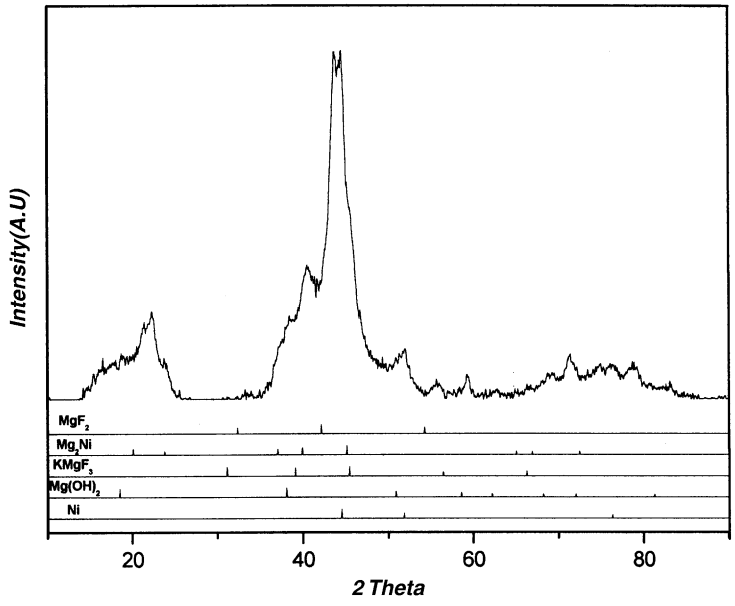

Fig. 9. XRD pattern of Mg_2Ni in 2F electrolyte.

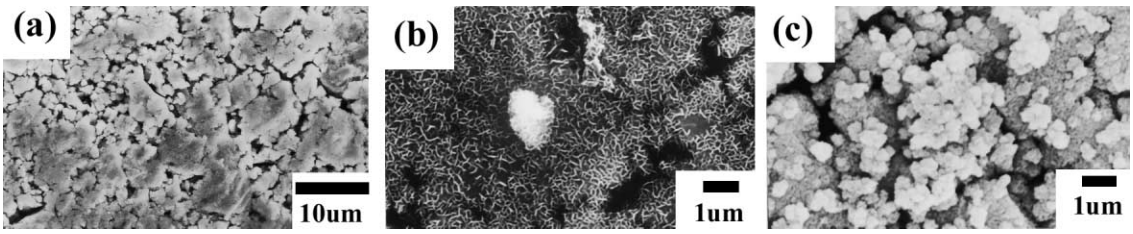

Fig. 10. SEM morphologies of Mg_2Ni electrode at (a) 0 cycle (2.000X), (b) 10 cycles in 2F electrolyte (8 000X), (c) 10 cycles in K electrolyte (10 000X).

The XRD patterns of electrodes in K electrolyte and 2F electrolyte after 10 cycles are given in Figs. 8 and 9, respectively. For electrolyte without the strong $Mg(OH)_2$ and Ni peaks appear as shown in the Fig. 8. By comparison with the data of Fig. 1, it is concluded that the Mg_2Ni phase disappears and a new $Mg(OH)_2$ phase is formed after 10 cycles. The $Mg(OH)_2$ peaks are relatively smaller when using an electrolyte with KF and peaks for MgF_2 are now observed, see Fig. 9.

The morphologies of the Mg_2Ni electrode surface before and after cycling in different electrolytes are given in Fig. 10. The electron micrographs show that the surface of the electrode before the test has a very fresh surface, Fig. 10(a). After 10 cycles (Fig. 10(b) and (c)) the $Mg(OH)_2$ phase covers the electrode surface. With a F^--containing electrolyte, however, the oxide content (determined by EDS mapping) is relatively lower. The surface structure has been said to have a rose-petal shape [13], which is also found for LaNi or $CaNi_5$ type metal hydrides by ex situ F-treatment. Therefore, it is concluded that in situ F-treatment by adding F^- ions can form a fluorination layer, MgF_2 on the surface of alloy and thus then improved the durability of the Mg_2Ni electrode.

In order to investigate further the effect of fluorination treatment of durability, the EIS of Mg_2Ni electrodes at 0 % DOD are as presented in Fig. 11. As the KF content is increased, the transfer resistance of the electrode is decreased. This implies that, for the nanocrystalline Mg_2Ni electrode in F^- containing electrolyte, both the charge transfer resistance of the hydrogen redox reaction on the

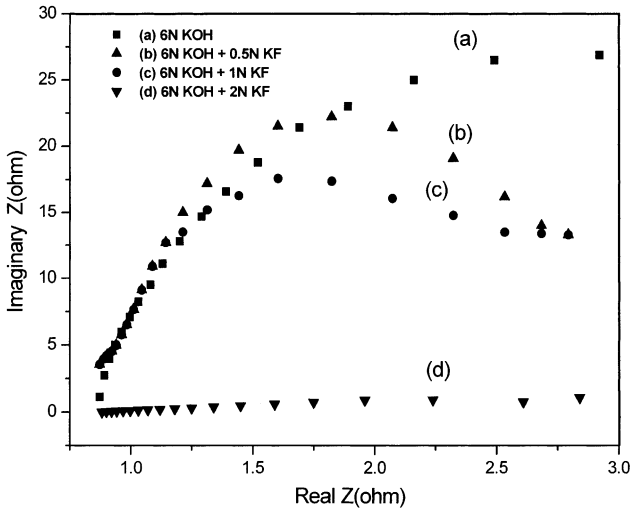

Fig. 11. Electrochemical impedance data of Mg_2Ni electrode in various electrolytes: (a) K electrolyte, (b) 0.5F electrolyte, (c) 1F electrolyte, (d) 2F electrolyte.

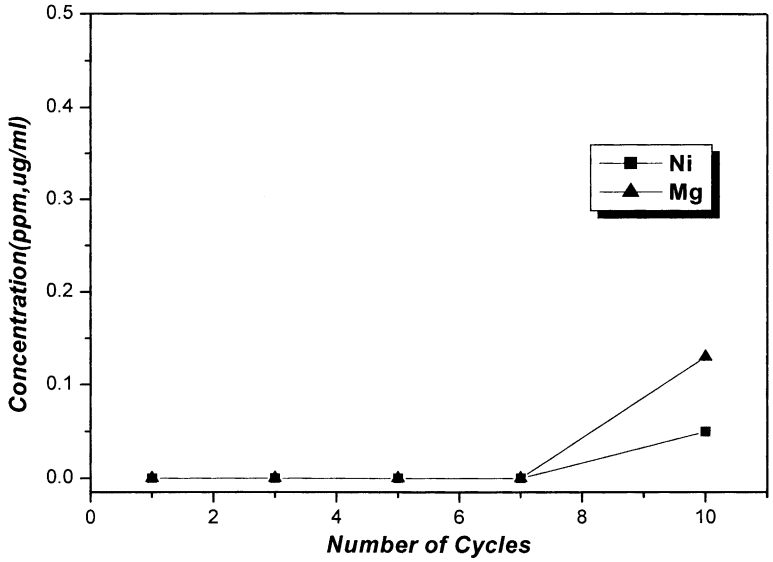

Fig. 12. ICP–AES data for electrolyte after 1, 3, 5, 7, and 10 cycles.

surface and the diffusion resistance of the hydrogen atom in the active metal are greatly reduced by F-treatment. It is concluded that the hydrogen reaction on the porous MgF_2 layer has lower transfer resistance compared with that on a $Mg(OH)_2$ layer.

The effect of F-treatment on the partial dissolution of the alloying elements of the electrode was investigated by ICP–AES. The amount of dissolution is a very small quantity (<13 ppm), as shown in Fig. 12. Therefore, loss of the metal hydride is negligible during F-treatment.

4. Conclusions

1. A nanocrystalline Mg_2Ni phase has been successfully synthesized after 20 h of ball-milling by a mechanical alloying method. The electrode has greatly improved charge–discharge characteristics, especially initial discharge capacity at low temperature.
2. Degradation of the electrode, which has good low-temperature characteristics, is still rapid because of the formation of a $Mg(OH)_2$ layer which hinders hydrogen diffusion at the surface.
3. It is suggested that the formation of $Mg(OH)_2$ can be accelerated at the active surface during the charge–discharge process. The surface is activated by volume expansion/shrinking of alloy, and by the formation of defects during the ball-milling process.
4. In situ F-treatment decreases the maximum discharge capacity, but the durability of the electrode is greatly improved.
5. Degradation of the Mg_2Ni electrode can be reduced by putting excess F^- ions in the electrolyte. Mg reacts with F^- ions rather than OH^- ions to form a thin, porous MgF_2 layer. This F_2 layer reduces charge–transfer resistance for the hydrogen reaction at the surface and also suppresses the formation of the $Mg(OH)_2$ layer, which is the main cause of electrode degradation.

Acknowledgements

The authors wish to acknowledge the financial support the Korea Research Foundation made in the program year of 1998.

References

[1] B. Knosp, L. Vallet, Ph. Blanchard, J. Alloys Compounds 293/295 (1999) 770.
[2] T. Sakai, I. Uehara, H. Ishikawa, J. Alloys Compounds 293/295 (1999) 762.
[3] N. Cui, B. Luan, H.K. Liu, S.X. Dou, J. Power Source 55 (1995) 263.
[4] N.H. Goo, J.H. Woo, K.S. Lee, J. Alloys Compounds 288 (1999) 286.
[5] J.P. Darnaudery, B. Darriet, M. Pezat, Int. J. Hydrogen Energy 8 (1983) 705.
[6] P. Sewan, B. Viswanathan, C.C. Swanny, V. Srinvasan, Int. J. Hydrogen Energy 13 (1998) 82.
[7] N. Cui, J.L. Luo, J. Alloys Compounds 265 (1998) 305.
[8] N. Cui, B. Luan, H.K. Liu, S.X. Dou, J. Power Source 63 (1996) 209.
[9] J.H. Woo, K.S. Lee, J. Electrochem. Soc. 146 (3) (1999) 819.
[10] H. Ishkawa, K. Oguru, A. Kato, H. Suzuki, E. Ishii, J. Less-Common Met. 120 (1) (1986) 123.
[11] T. Sakai, H. Ishikawa, K. Oguru, C. Iwakura, H. Yoneyama, J. Electrochem. Soc. 134 (3) (1997) 558.
[12] F.J. Liu, S. Suda, J. Alloys Compounds 190 (1) (1992) 57.
[13] F.J. Liu, S. Suda, J. Alloys Compounds 231 (1995) 742.
[14] M. Sakashita, Z.P. Li, S. Suda, J. Alloys Compounds 253/254 (1997) 500.
[15] M. Kanda, J. Alloys Compounds 253/254 (1997) 660.
[16] N. Cui, B. Luan, H.J. Zhao, J. Alloys Compounds 233 (1996) 236.
[17] L. Yongning, Z. Xianji, J. Alloys Compounds 267 (1998) 231.
[18] K.J. Gross, D. Cahartouni, E. Leroy, A. Zuttel, L. Schlapbach, J. Alloys Compounds 269 (1998) 259.
[19] D. Cracco, A. Percheron-Guegan, J. Alloys Compounds 268 (1998) 248.
[20] B.D. Culity, Elements of X-ray Diffraction, 2nd Edition, Addison-Wesley, Reading, MA, 1978, p. 101.
[21] N. Cui, J.L. Luo, J. Alloys Compounds 231 (1995) 397.
[22] Z.P. Li, S. Suda, in: P.D. Bennett, T. Sakai (Eds.), Hydrogen and Metal Hydride Batteries, The Electrochemical Society, (1995) 78.
[23] I. Barin, Thermochemical Data of Pure Substances, VCH, New York, 1989.
[24] M. Purbaix, Atlas of Electrochemical Equilibria in Aqueous Solutions, Pergamon Press, Oxford, New York, 1966.